This article has been accepted for publication in a future issue of this journal, but has not been fully edited. Content may change prior to final publication. Citation information: DOI 10.1109/LWC.2019.2906184, IEEE Wireless Communications Letters

Detection and Analysis of Symbol-Asynchronous Uplink NOMA with Equal Transmission Power

Jingmin Liu, Ying Li, *Member, IEEE,* Guanghui Song, *Member, IEEE,* and Yue Sun

***Abstract*—We consider a symbol-asynchronous uplink non-orthogonal multiple access (NOMA) model with equal-power transmission, where K users transmit their codewords to a common receiver in an asynchronous manner. The received signal vector is an asynchronous superposition of all users' codewords. Due to the equal-power transmission, such signal detection scheme as successive interference cancellation (SIC) is invalid. We propose a message passing (MP) detection for the symbol-asynchronous NOMA system and analyze its performance by deriving a signal-to-interference-plus-noise ratio (SINR) of the detector output. Our analysis and simulations show that symbol asynchronization, i.e., each user has a different transmission time offset, in fact benefits signal detection, and its performance depends on the employed modulation waveform.**

***Index Terms*—Symbol-asynchronous, non-orthogonal multiple access (NOMA), message passing (MP) detection.**

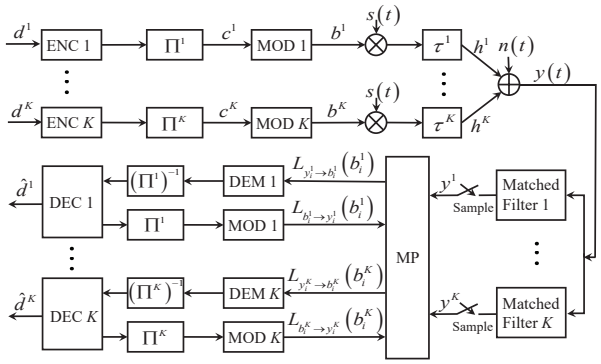

Fig. 1: Symbol-asynchronous NOMA system (ENC: encoder, DEC: decoder, MOD: modulator, DEM: Demodulator).

I. Introduction

Non-orthogonal multiple access (NOMA) is proposed as a promising technology to handle such explosive data traffic by supporting multiple transmissions using the same wireless resources [1]. NOMA techniques can be roughly categorized into two main classes: power-domain NOMA and code-domain NOMA. For the power-domain NOMA, users are allocated with different power, and at the receiver, a successive interference cancellation (SIC) detection scheme is employed to detect each user's signal [2]. For the code-domain NOMA, users can be allocated with the same transmission power, and massage-passing (MP) signal detection schemes are employed for their signal detections at the receiver. Examples of code-domain NOMA schemes are interleave division multiple access (IDMA) [3] [4], sparse code multiple access (SCMA) [5], and pattern division multiple access (PDMA) [6] [7].

Most of these works [3]–[7] assume strict symbol-synchronization at the receiver, i.e., the beginnings of each user's signal are guaranteed to coincide. This requires accurate user cooperation and will reduce data transmission efficiency significantly. Work [8] considered symbol-asynchronous NOMA with unequal power transmission and developed a triangular SIC detection scheme.

In this paper, we consider signal detection and performance analysis for symbol-asynchronous NOMA with equal power transmission. We propose an MP detection for this system that is an extension of conventional MP detections for symbol-synchronous systems. Different from conventional works [3]–[7], due to asynchronization, the matched filter output is a superposed signal of different users across two adjacent time slots, so the factor graph cannot be illustrated in a two-dimensional way. To illustrate the relation between the received signal and signals of different users, we propose a three-dimensional factor graph representation for it, and develop a cross-slot MP detection scheme, while the conventional MP detection for symbol-synchronous NOMA, known as elementary signal estimator (ESE) [3]–[7], is performed only among users within each time slot. We analyze the signal-to-interference-plus-noise ratio (SINR) of the detector output and show that the MP detection performance of symbol-asynchronous NOMA is significantly affected by an auto-correlation property of the employed modulation waveform. We show that with different user transmission time offset, symbol-asynchronous NOMA achieves an even better detection performance than symbol-synchronous systems.

II. System Model

Fig.1 shows an equal-power symbol-asynchronous uplink NOMA system. The length-n message vector $\boldsymbol{d}^k = (d_1^k, \ldots, d_n^k), d_i^k \in \{0, 1\}$, of user k is first encoded to a length-l codeword through encoder-k, $k = 1, \cdots, K$. So the rate of user-k is $R_k = n/l$. Interleaver Π^k is employed by user k to permute the location of each coded bit as in the IDMA system

Manuscript received September 1, 2018; revised November 28, 2018; accepted March 9, 2019. Date of publication *, *; date of current version *, *. This work was supported in part by the Key Industry Innovation Chain Project of Shaanxi under Grant 2018ZDCXLGY-04-04, and in part by the National Natural Science Foundation of China under Grant 61671345. The associate editor coordinating the review of this paper and approving it for publication was *. *(Corresponding author: Ying Li.)*

J. Liu, Y. Li and Y. Sun are with the State Key Lab of Integrated Services Networks, Xidian University, Xi'an, 710071, China (e-mail: jingminliu0@gmail.com; yli@mail.xidian.edu.cn; ysun@mail.xidian.edu.cn).

G. Song is with the Intelligent Information Engineering and Sciences Department, Doshisha University, Kyoto 610-0321, Japan (e-mail: ghsong2008@hotmail.com).

This article has been accepted for publication in a future issue of this journal, but has not been fully edited. Content may change prior to final publication. Citation information: DOI 10.1109/LWC.2019.2906184, IEEE Wireless Communications Letters

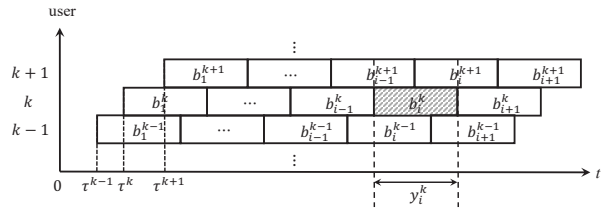

Fig. 2: Interference of b_i^k in a K-user symbol-asynchronous NOMA transmission system.

[3]. After interleaving, the obtained sequence $\boldsymbol{c}^k$ is modulated to $\boldsymbol{b}^k=(b_1^k,\ldots,b_p^k)$ through an quadrature phase shift keying (QPSK) modulator, where $p=l/2$, and l is assumed to be an even number. Then each user transmits a modulated symbol by sending signal $b_i^k s(t-(i-1)T)$, where $s(t)$ is an unitary-energy signal waveform with $\int_0^T s^2(t)dt=1$ and vanishing outside interval $[0,T]$, where T is the symbol period. All the users utilize the same $s(t)$ that is known to the receiver.

In this paper, we focus on the asynchronous NOMA system, where each user can have a different arriving time at the receiver. Let τ^k be the time offset of user k. We assume the receiver knows the offsets $\tau^k,\forall k$. Without loss of generality, we assume symbol-asynchronous NOMA with $0=\tau^1\leq\cdots\leq\tau^K<T$. Note that when $\tau^k>T$, the system becomes a frame-asynchronous system. In this paper, we assume that frame synchronization is achieved since it is much easier to realize than symbol synchronization. In practical communication, symbol synchronization among different users is more difficult to achieve owing to the much smaller time scale involved [10].

Rayleigh fading channel is considered, i.e., $h^k\sim CN(0,1)$, and we assume that the receiver knows the perfect channel coefficient h^k, $\forall k$. Let $n(t)$ be the white Gaussian noise with two-side power spectral density $N_0/2$. The received signal is

$$y(t)=\sum_{k=1}^{K}\sum_{i=1}^{p}h^k b_i^k s(t-(i-1)T-\tau^k)+n(t).$$

We utilize a user-oriented matched filter to project $y(t)$ in the direction of $s\left(t-(i-1)T-\tau^k\right)$

$$\begin{aligned}y_i^k&=\int_{(i-1)T+\tau^k}^{iT+\tau^k}y(t)s\left(t-(i-1)T-\tau^k\right)dt\\&=h^k b_i^k+\sum_{m<k}h^m\left(\rho_{\tau^k-\tau^m}b_i^m+\rho_{T-(\tau^k-\tau^m)}b_{i+1}^m\right)\\&\quad+\sum_{m>k}h^m\left(\rho_{T-(\tau^m-\tau^k)}b_{i-1}^m+\rho_{\tau^m-\tau^k}b_i^m\right)+n_i^k\end{aligned}\quad(1)$$

where ρ_τ is an auto-correlation $\rho_\tau=\int_0^T s(t-\tau)s(t)dt$.

From Fig.2 and equation (1), we notice that, due to symbol asynchronization, b_i^k is interfered by not only b_i^m but also b_{i-1}^m or b_{i+1}^m for $m\neq k$. When $\tau^k=0,\forall k$, since $\rho_0=1$ and $\rho_T=0$, (1) becomes $y_i^k=\sum_{j=1}^{K}h^j b_i^j+n_i^k$, which is the symbol asynchronous case.

III. MP Detection

In this section, we propose an MP detection for the symbol-asynchronous NOMA system.

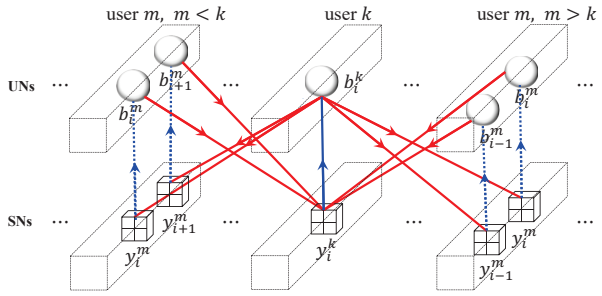

Fig. 3: Three-dimensional factor graph representation of MP detection for the K-user symbol-asynchronous NOMA.

The MP detection is performed on factor graph, which is utilized to represent the relation between transmitted symbols and output symbols of the matched filter Different from conventional works [3]–[7], due to symbol asynchronization, the matched filter output is a superposed signal of different users across two consecutive time slots (1), so the factor graph cannot be illustrated in a two-dimensional way. To illustrate the relation between matched filter output and signals of different users, we propose a three-dimensional factor graph representation for the asynchronous NOMA system in Fig.3, based on which we develop a cross-slot MP detection.

In the factor graph, the transmitted symbols $b_i^k,\forall i,\forall k$ are denoted as user nodes (UNs), and matched filter outputs $y_i^k,\forall i,\forall k$ are denoted as sum nodes (SNs). According to (1), since y_i^k is a superposed signal of symbols b_i^m, $b_{i+1}^m, m<k$ and $b_{i-1}^m, m>k$, so there is an edge between SN y_i^k and each of these UNs. Different from conventional factor graphs [3]–[7], edges are directed so that the message over each edge is propagated unidirectionally.

The MP detection is iteratively conducted between SNs and UNs on the factor graph, where the log-likelihood ration (LLR) is propagated over the edges. In each iteration, each SN and UN should process once. For example, SN y_i^k should calculate an LLR about b_i^k based on received signal y_i^k and the incoming LLRs from UNs and delivers it to UN b_i^k. Different from [3]–[7], the processing at UN b_i^k is quit simple, which only needs to broadcast its acquired message (from SN y_i^k) to each of its outgoing edges.

In the following, we focus on the processing at SN y_i^k, LLR calculation of b_i^k, to show our MP detection. Since b_i^k is a complex QPSK symbol, the detection for its real part $\mathrm{R}(b_i^k)$ and its imaginary part can be similarly. Let $\bar{h}^k$ and $|h^k|$ be the conjugate and modulus of h^k, respectively. Denote $\tilde{h}^m=\bar{h}^k h^m/|h^k|$. We multiply $\bar{h}^k/|h^k|$ on both side of (1) and obtain

$$(y_i^k)'=\bar{h}^k/|h^k|y_i^k=|h^k|b_i^k+\alpha_i^k+\bar{h}^k/|h^k|n_i^k\quad(2)$$

where

$$\begin{aligned}\alpha_i^k&=\sum_{m<k}\tilde{h}^m\left(\rho_{\tau^k-\tau^m}b_i^m+\rho_{T-(\tau^k-\tau^m)}b_{i+1}^m\right)\\&\quad+\sum_{m>k}\tilde{h}^m\left(\rho_{T-(\tau^m-\tau^k)}b_{i-1}^m+\rho_{\tau^m-\tau^k}b_i^m\right)\end{aligned}$$

This article has been accepted for publication in a future issue of this journal, but has not been fully edited. Content may change prior to final publication. Citation information: DOI 10.1109/LWC.2019.2906184, IEEE Wireless Communications Letters

is the interference (from other users) of b_i^k. Here we approximate $(y_i^k)'$ as a complex Gaussian variable by the central limit theorem [3], and its real part has the distribution

$$p\left(\mathrm{R}((y_i^k)')\left|\mathrm{R}(b_i^k)=\pm 1\right.\right) = \frac{1}{\sqrt{2\pi\left(V_{\mathrm{R}}[\alpha_i^k]+\frac{N_0}{2}\right)}}\exp\left(\frac{-\left(\mathrm{R}((y_i^k)')-\left(\pm|h^k|+E_{\mathrm{R}}[\alpha_i^k]\right)\right)^2}{2\left(V_{\mathrm{R}}[\alpha_i^k]+\frac{N_0}{2}\right)}\right)$$

where $E_{\mathrm{R}}[\alpha_i^k]$ and $V_{\mathrm{R}}[\alpha_i^k]$ are mean and variance of $\mathrm{R}(\alpha_{\mathrm{i}}^{\mathrm{k}})$, respectively. Thus, the LLR of $\mathrm{R}\left(b_i^k\right)$ is

$$\begin{aligned} L_{y_i^k\to b_i^k}\left(\mathrm{R}(b_i^k)\right) &= \log\frac{p\left((y_i^k)'\left|\mathrm{R}(b_i^k)=+1\right.\right)}{p\left((y_i^k)'\left|\mathrm{R}(b_i^k)=-1\right.\right)} \\ &= 2|h^k|\frac{\mathrm{R}((y_i^k)')-E_{\mathrm{R}}[\alpha_i^k]}{V_{\mathrm{R}}[\alpha_i^k]+\frac{N_0}{2}} \end{aligned} \tag{3}$$

where $E_{\mathrm{R}}[\alpha_i^k]$ and $V_{\mathrm{R}}[\alpha_i^k]$ are calculated as

$$\begin{aligned} E_{\mathrm{R}}[\alpha_i^k] = &\sum_{m<k}\Big(\rho_{\tau^k-\tau^m}(\mathrm{R}(\tilde{h}^m)E_{\mathrm{R}}[b_i^m]-\mathrm{I}(\tilde{h}^m)E_{\mathrm{I}}[b_i^m]) \\ &+\rho_{T-(\tau^k-\tau^m)}(\mathrm{R}(\tilde{h}^m)E_{\mathrm{R}}[b_{i+1}^m]-\mathrm{I}(\tilde{h}^m)E_{\mathrm{I}}[b_{i+1}^m])\Big) \\ &+\sum_{m>k}\Big(\rho_{\tau^m-\tau^k}(\mathrm{R}(\tilde{h}^m)E_{\mathrm{R}}[b_i^m]-\mathrm{I}(\tilde{h}^m)E_{\mathrm{I}}[b_i^m]) \\ &+\rho_{T-(\tau^m-\tau^k)}(\mathrm{R}(\tilde{h}^m)E_{\mathrm{R}}[b_{i-1}^m]-\mathrm{I}(\tilde{h}^m)E_{\mathrm{I}}[b_{i-1}^m])\Big) \end{aligned}$$

$$\begin{aligned} V_{\mathrm{R}}\left[\alpha_i^k\right] = &\sum_{m<k}\Big(|\rho_{\tau^k-\tau^m}|^2(\mathrm{R}(\tilde{h}^m)^2V_{\mathrm{R}}[b_i^m]+\mathrm{I}(\tilde{h}^m)^2V_{\mathrm{I}}[b_i^m]) \\ &+|\rho_{T-(\tau^k-\tau^m)}|^2(\mathrm{R}(\tilde{h}^{m^2}V_{\mathrm{R}}[b_{i+1}^m]+\mathrm{I}(\tilde{h}^m)^2V_{\mathrm{I}}[b_{i+1}^m])\Big) \\ &+\sum_{m>k}\Big(|\rho_{\tau^m-\tau^k}|^2(\mathrm{R}(\tilde{h}^m)^2V_{\mathrm{R}}[b_i^m]+\mathrm{I}(\tilde{h}^m)^2V_{\mathrm{I}}[b_i^m]) \\ &+|\rho_{T-(\tau^m-\tau^k)}|^2(\mathrm{R}(\tilde{h}^m)^2V_{\mathrm{R}}[b_{i-1}^m]+\mathrm{I}(\tilde{h}^m)^2V_{\mathrm{I}}[b_{i-1}^m])\Big) \end{aligned}$$

where the means and variances of $b_i^m, m\neq k, b_{i+1}^m, m<k$, and $b_{i-1}^m, m>k$, can be calculated based on the incoming messages from UNs as

$$\begin{aligned} E_{\mathrm{R}}[b_i^m] &= \tanh(L_{b_i^m\to y_i^k}(\mathrm{R}(b_i^m))/2) \\ V_{\mathrm{R}}[b_i^m] &= 1-E_{\mathrm{R}}^2[b_i^m] \end{aligned}$$

where we used the relation between variable's LLR and its mean. $E_{\mathrm{I}}[b_i^m]$, and $V_{\mathrm{I}}[b_i^m]$ can be calculated similarly. At the first iteration, $L_{b_i^m\to y_i^k}(\mathrm{R}(b_i^m))$ should be initialized to 0.

The processing at a UN is very simple. After receiving $L_{y_i^k\to b_i^k}\left(\mathrm{R}(b_i^k)\right)$, UN b_i^k just forwards this message over each of its outgoing edge for the next round of SN processing.

Conventional ESE for symbol-synchronous NOMA [3]–[7] is a special case of our detection scheme when $\tau^k=0,\forall k$ leading to $\rho_{\tau^m-\tau^k}=1$ and $\rho_{T-(\tau^m-\tau^k)}=0$.

The complexity of our MP is $O(K)$ which only linearly increases as the user number increases. However, the computation complexity of conventional LMMSE detection is $O(K^3)$, where $O(K^3)$ arises from the calculation of matrix inverse. Note that MP detection has higher complexity than the conventional SIC detection for NOMA systems. However, since SIC relies on unequal-power transmission, it can not be applied here due to our equal power assumption.

IV. SINR Analysis

In this section, we analyze an SINR property of SN processing and theoretically show that asynchronous NOMA system can has even better detection performance than synchronous NOMA system.

Applying (2) in (3), we obtain

$$\begin{aligned} L_{y_i^k\to b_i^k}(\mathrm{R}(b_i^k)) = &\frac{2|h^k|}{V_{\mathrm{R}}[\alpha_i^k]+\frac{N_0}{2}}\left(|h^k|\mathrm{R}(b_i^k)\right. \\ &\left.+\mathrm{R}(\alpha_i^k)-E_{\mathrm{R}}[\alpha_i^k]+\mathrm{R}(\bar{h}^k n_i^k)/|h^k|\right) \end{aligned} \tag{4}$$

where $|h^k|\mathrm{R}(b_i^k)$ is the useful signal, and $\mathrm{R}(\alpha_i^k)-E_{\mathrm{R}}[\alpha_i^k]+\mathrm{R}(\bar{h}^k n_i^k)/|h^k|$ contains residual interference from the other users and noise. Average SINR of SN output is calculated as

$$\begin{aligned} \mathrm{SINR}_k^{asy} &= \frac{E\left[|h^k|^2|\mathrm{R}(b_i^k)|^2\right]}{E\left[|\mathrm{R}(\alpha_i^k)-E_{\mathrm{R}}[\alpha_i^k]+\mathrm{R}(\bar{h}^k n_i^k)|^2\right]} \\ &= \frac{|h^k|^2}{E[V_{\mathrm{R}}[\alpha_i^k]]+\frac{N_0}{2}} \end{aligned} \tag{5}$$

where we used $|\mathrm{R}(b_i^k)|=1$. Using the facts that $|h^m|=|\tilde{h}^m|$, and $E[V_{\mathrm{R}}[b_j^m]]=E[V_{\mathrm{I}}[b_j^m]], j=i-1,i,i+1$, $E[V_{\mathrm{R}}[b_{i-1}^m]]=E[V_{\mathrm{R}}[b_i^m]]=E[V_{\mathrm{R}}[b_{i+1}^m]]\triangleq\bar{V}_b^m$ since they have the same distribution, $E[V_{\mathrm{R}}[\alpha_i^k]]$ in (5) is calculated as

$$E[V_{\mathrm{R}}[\alpha_i^k]]=\sum_{m\neq k}(\rho^2_{|\tau^k-\tau^m|}+\rho^2_{T-|\tau^k-\tau^m|})|h^m|^2\bar{V}_b^m.$$

Note that $\bar{V}_b^m$ is an average variance of each bit in the previous processing. Thus, we obtain the average SINR of an SN output

$$\mathrm{SINR}_k^{asy}=\frac{|h^k|^2}{\sum_{m\neq k}(\rho^2_{|\tau^k-\tau^m|}+\rho^2_{T-|\tau^k-\tau^m|})|h^m|^2\bar{V}_b^m+\frac{N_0}{2}}.$$

Especially, when $\tau_1=\tau_2=\cdots=\tau_K$, the SINR function degrades to the synchronous case of ESE detection [3]–[7]

$$\mathrm{SINR}_k^{sy}=\frac{|h^k|^2}{\sum_{m\neq k}|h^m|^2\bar{V}_b^m+\frac{N_0}{2}}.$$

Applying Cauchy-Schwarz inequality, we have

$$\begin{aligned} &\rho^2_{|\tau^k-\tau^m|}+\rho^2_{T-|\tau^k-\tau^m|} \\ &<\int_0^T[s(t-|\tau^k-\tau^m|)]^2dt\int_0^T[s(t)]^2dt \\ &\quad+\int_0^T[s(t+(T-|\tau^k-\tau^m|))]^2dt\int_0^T[s(t)]^2dt=1. \end{aligned}$$

Therefore, $\mathrm{SINR}_k^{asy} > \mathrm{SINR}_k^{sy}$ holds, which means MP detection of asynchronous NOMA systems theoretically outperforms that of synchronous systems.

It should be emphasized that the SINR of MP detection for asynchronous NOMA is significantly determined by the auto-correlation property of the employed modulation waveform, i.e., by the term $\rho^2_{|\tau^k-\tau^m|}+\rho^2_{T-|\tau^k-\tau^m|}$ in SINR_k^{asy} expression, while for synchronous case, signal waveform has no affect on it. In Fig. 4, we illustrate some examples of modulation waveforms and their auto-correlation property $\rho_\tau^2+\rho_{T-\tau}^2, \tau=|\tau^k-\tau^m|$. The expected value $E[\rho_\tau^2+\rho_{T-\tau}^2]$ when the two time offsets τ^k,τ^m are independently and uniformly distributed on $[0,T]$ is also demonstrated. The waveform with lower

This article has been accepted for publication in a future issue of this journal, but has not been fully edited. Content may change prior to final publication. Citation information: DOI 10.1109/LWC.2019.2906184, IEEE Wireless Communications Letters

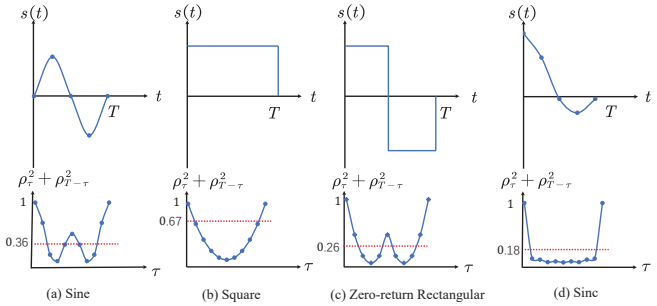

Fig. 4: Modulation symbol waveforms $s(t)$ and their auto-correlation property $\rho_\tau^2+\rho_{T-\tau}^2$ (below each waveform). Dashed lines demonstrate the expected value $E[\rho_\tau^2+\rho_{T-\tau}^2]$ for random time offsets with uniform distribution.

$E[\rho_\tau^2+\rho_{T-\tau}^2]$ may have a better SINR property, and better MP detection performance, due to lower user interference.

V. Simulation Results

In this section, we compare the BER performances of our MP detection for the asynchronous NOMA system with that of ESE detection for the synchronous NOMA system. We also compare our detection scheme with conventional LMMSE detection for both synchronous and asynchronous systems.

Fig.5 gives the simulation results of the BER performances for 3-user and 10-user NOMA models. The Sine waveform and Square waveform, i.e., waveform (a) and (b) in Fig. 4, are employed for symbol-asynchronous NOMA over the fast Rayleigh fading channel. The time offset of each user is randomly and uniformly distributed on $[0, T]$. For symbol-synchronous case, the waveform can be any unitary energy waveform with $\int_0^T s^2(t)dt = 1$, which does not affect its detection performance. We employ the regular repeat-accumulate (RA) code serially concatenated with repetition code as the channel coding for each user, and QPSK modulation is adopted. The coding rates of RA, repetition codes are $1/2$, $1/3$ for 3-user NOMA, and $1/4$, $1/3$ for 10-user NOMA. In these simulations, the information length of each user is 4096, and the number of decoding iterations is 50. The complexity of LMMSE detection becomes very high when the user number is large, so we only provide the simulation results of LMMSE detection with 3 users.

BER performance of MP detection is almost the same as that of LMMSE detection even though MP detection has much lower complexity. BER performance of asynchronous NOMA systems always outperforms that of synchronous NOMA, no mater whether the MP or LMMSE detection is applied. For 3-user NOMA, MP detection for the asynchronous system can achieve performance gain of about 0.18dB at BER$= 10^{-4}$ over the synchronous case. As the user number is larger, this gain is more obvious. For 10-user NOMA, asynchronous system has 1.76dB and 1.37dB gains, when the Sine and the Square waveform are employed, respectively, over synchronous ESE. Sine waveform always outperforms Square waveform due to its better auto-correlation property as revealed in Fig. 4.

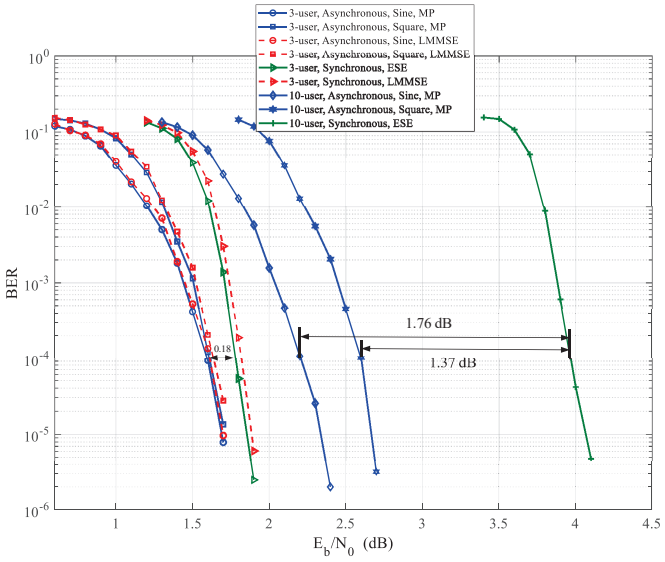

Fig. 5: BER performances of asynchronous NOMA and synchronous NOMA over fast Rayleigh fading channels with different detection schemes.

VI. Conclusion

We considered signal detection and performance analysis for the asynchronous NOMA system with equal transmission power and proposed a cross-slot MP detection that can efficiently deal with user interference. Analysis and simulations show that the proposed MP detection can even outperforms that of synchronous NOMA.

References

[1] L. Dai, B. Wang, Y. Yuan, S. Han, C.L. I, and Z. Wang, "Non-orthogonal multiple access for 5G: Solutions, challenges, opportunities, and future research trends," *IEEE Commun. Mag.*, vol. 53, no. 9, pp. 74-81, Sep. 2015.

[2] Z. Ding, P. Fan, and H.V. Poor, "Impact of user pairing on 5g nonorthogonal multipleaccess downlink transmissions," *IEEE Trans. Veh. Tech.*, vol.65 no.8, pp. 6010-6023, Aug. 2016.

[3] P. Li, L. H. Liu, K. Y. Wu, and W. K. Leung, "Interleaving-division multiple-access," *IEEE Trans. Wireless Commun.*, vol. 5, no. 4, pp. 938-947, Apr. 2006.

[4] G. Song, X. Wang, and J. Cheng, "A low-complexity multiuser coding scheme with near-capacity performance," *IEEE Trans. Veh. Tech.*, vol. 66, no.8, pp. 6775-6786, Aug. 2017.

[5] H. Nikopour and H. Baligh, "Sparse code multiple access," in *Proc. IEEE PIMRC 2013*, pp. 332-336, Sept. 8-11.

[6] X. Dai, S. Chen, S. Sun, S. Kang, Y. Wang, Z. Shen, and J. Xu, "Successive interference cancelation amenable multiple access (SAMA) for future wireless communications," (invited paper) in *Proc. IEEE ICCS 2014*, pp. 222-226, Nov. 12-15.

[7] X. Dai, Z. Zhang, S. Chen, S.Sun, and B. Bai, "Pattern division multiple access (PDMA): a new multiple access technology for 5G," *IEEE Wireless Commun.*, vol. 25, no. 2, pp. 54-60, Apr. 2018.

[8] H. Haci, H. Zhu, and J. Wang, "Performance of non-orthogonal multiple access with a novel asynchronous interference cancellation technique," *IEEE Trans. Commun.*, vol. 65, no. 3, pp. 1319-1335, Mar. 2017.

[9] P. Li, L. Liu, K.Wu, and W. Leung, "Approaching the capacity of multiple access channels using interleaved low-rate codes," *IEEE Commun. Lett.*, vol. 8, no. 1, pp. 4-6, Jan. 2004.

[10] S. Verdù, "The capacity region of the symbol-asynchronous Gaussian multiple-access channel," *IEEE Trans. Inform. Theory*, vol. 35, no. 4, pp. 733-751, Apr. 1989.